

Report on "Self-directed Joint Research" of MERIT program

## **Mathematical study on the extended PXP model and quantum many-body scar states**

Naoyuki Shibata<sup>1</sup>, Norifumi Matsumoto<sup>2</sup>

<sup>1</sup> *Department of Physics, Graduate School of Science, Katsura Lab.*

<sup>2</sup> *Department of Physics, Graduate School of Science, Ueda Lab.*

### **【Authors】**

**Naoyuki Shibata** is engaging in theoretical studies on quantum many-body systems, especially on integrable systems, open quantum systems, and quantum many-body scar states. In this study, N. Shibata is responsible for numerical calculation.

**Norifumi Matsumoto** is engaging in theoretical studies on open non-equilibrium systems, especially on quantum phase transitions and critical phenomena in open systems. In this study, N. Matsumoto is responsible for mathematical analysis.

### **【Abstract】**

In recent years, unusual states called quantum many-body scar states in isolated quantum many-body systems have been actively studied theoretically and experimentally. Such states exhibit an anomalously slow thermalization or even absence of it despite the absence of an extensive number of conserved quantity. In this study, we investigate an influence of the hopping degree of freedom on quantum many-body scar states in the Rydberg-atom chain, in which such unconventional states were experimentally discovered for the first time. As a result, we find that adding the hopping degree of freedom gives rise to new quantum many-body scar states and, consequently, new initial states exhibiting the absence of thermalization. Furthermore, we clarify the concrete expressions of some simple quantum many-body scar states. This work provides insights into quantum many-body scar states and thermalization from a general point of view.

## 【Introduction : Thermalization and quantum many-body scar states】

### (1) Thermalization in isolated quantum many-body systems

In recent years, the development of experimental techniques such as cold-atom systems has led to the experimental realization of quantum many-body systems isolated from the environment. Furthermore, thermalization in such isolated quantum systems has been experimentally observed [1]. In Ref. [1], it is reported that the particle-number density in a cold-atom system trapped in an optical lattice relaxes to the thermal equilibrium expectation value when tunneling among sites turns on for an initial state in the form of a density wave (Fig. 1).

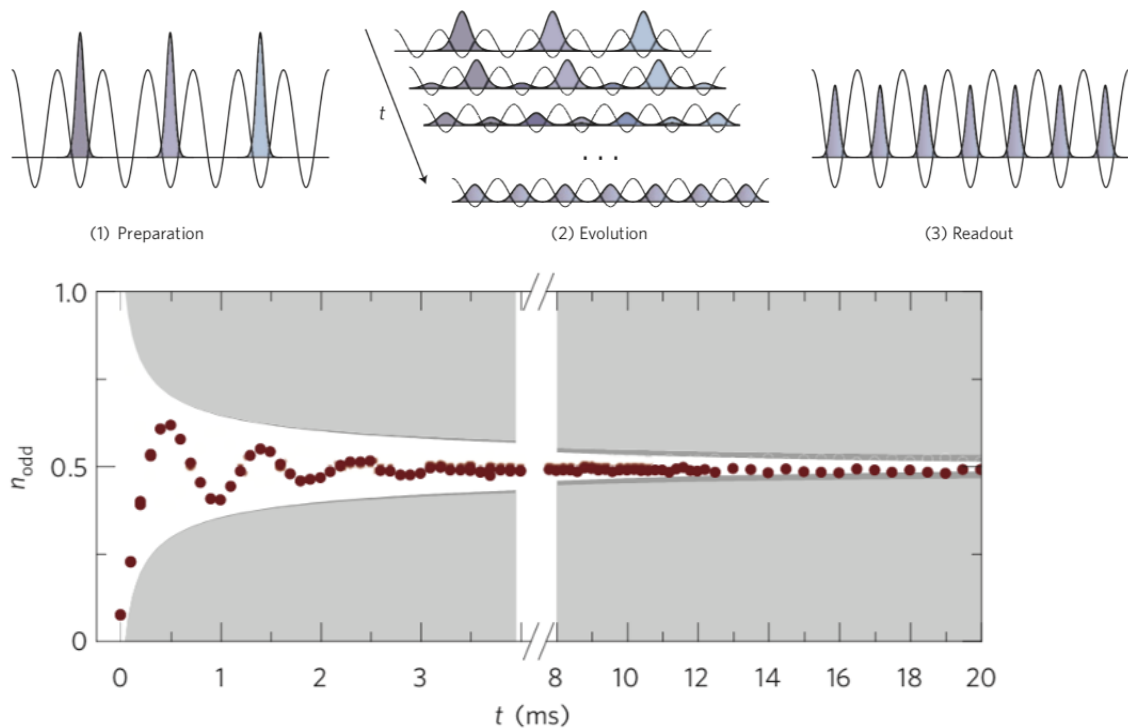


**Fig. 1** : Thermalization in an isolated cold-atom system. The particle-number density in a cold-atom system trapped in an optical lattice relaxes to the thermal equilibrium expectation value when tunneling among sites turns on for an initial state in the form of a density wave. Reproduced from Ref. [1].

In such dynamics, since the initial state is a pure state and the time evolution is unitary, the whole system remains in a pure state even after the time evolution. In statistical mechanics, in contrast, the thermal-equilibrium state in an isolated system is described by a mixed state called the microcanonical ensemble. Here, the eigenstate thermalization hypothesis (ETH) [2] explains the consistency of these seemingly contradictory facts.

## (2) Eigenstate thermalization hypothesis (ETH)

The eigenstate thermalization hypothesis (ETH) [2] states that the expectation value of a local observable for an energy eigenstate in an energy shell with a small width coincides with the thermal-equilibrium expectation value in the thermodynamic limit. In particular, the "strong ETH," which states that all the energy eigenstates in the energy shell satisfy the ETH, is a sufficient condition for thermalization.

It has long been believed that the strong ETH holds and that arbitrary initial states exhibit thermalization in general non-integrable systems [3], which do not have an extensive number of conserved quantity. Recently, however, a counterexample to this general expectation has been discovered in an experiment with a Rydberg-atom chain [4]. Such unusual states called quantum many-body scar states have attracted widespread attention.

## (3) Quantum many-body scar state

Quantum many-body scar states [4] are unusual states in isolated quantum many-body systems, which exhibit an anomalously slow thermalization or even the absence of it despite the absence of an extensive number conserved quantity. Such states were first experimentally discovered in a cold-atom system trapped in an optical lattice [4]. This system is effectively described by the PXP model in a two-level system [5], in which transitions occur between the ground level and a higher-energy level called the Rydberg level within each atom and neighboring atoms in the Rydberg level feel a strong repulsion with one another. In this system, most of the initial states quickly relax to the thermal equilibrium, but it was pointed out that the thermalization is anomalously slow when certain states, such as a  $Z_2$  density-wave state, are chosen as an initial state (Fig. 2).

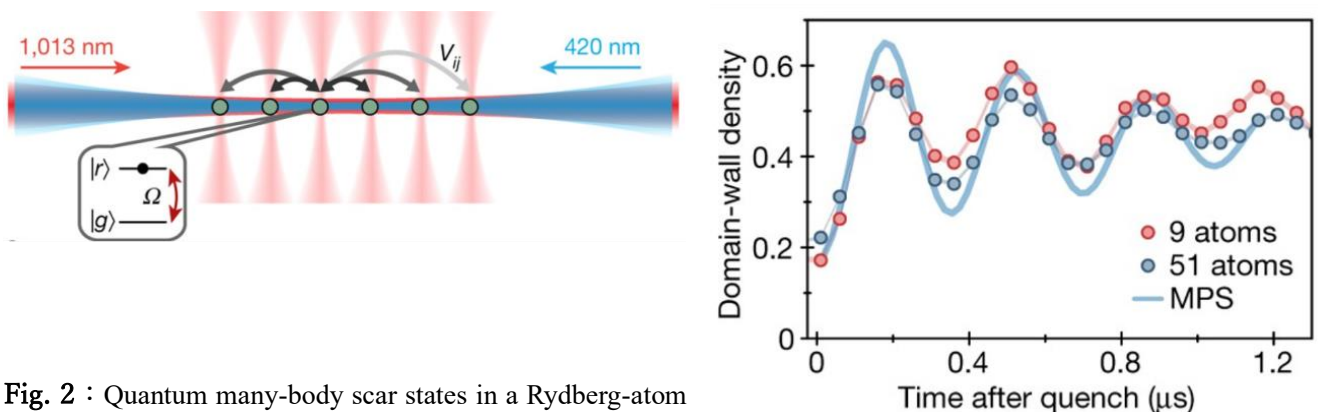


Fig. 2 : Quantum many-body scar states in a Rydberg-atom chain. The thermalization is anomalously slow when certain states, such as a  $Z_2$  density-wave state, are chosen as an initial state. Reproduced from Ref. [4].

### 【Aim of research】

This research aims to investigate emergent dynamics in a cold-atom system trapped in an optical lattice with a competition between a thermalization induced by tunneling and a contribution of quantum many-body scar states arising from the Rydberg interaction. This study provides insights into the emergence of quantum many-body scar states and thermalization from a general point of view.

### 【Model】

In this study, to achieve the above goal, we investigate the influence on quantum many-body scar states by introducing the hopping degrees of freedom into atoms in the Rydberg-atom chain (Fig. 3), in which quantum many-body scar states were first experimentally discovered. Specifically, we consider a system of hard-core bosonic atoms on a one-dimensional lattice, where each atom is described as a two-level system consisting of a ground-state level  $g$  and the Rydberg level  $r$ . The Hamiltonian is given as follows:

$$\begin{aligned} H &= H_g + H_r + H_{\text{Rabi}}, \\ H_g &= -J_g \sum_j (b_{j+1,g}^\dagger b_{j,g} + b_{j,g}^\dagger b_{j+1,g}), \\ H_r &= -J_r \sum_j P_{j-1} (b_{j+1,r}^\dagger b_{j,r} + b_{j,r}^\dagger b_{j+1,r}) P_{j+2}, \\ H_{\text{Rabi}} &= \Omega P_{j-1} (b_{j,r}^\dagger b_{j,g} + b_{j,g}^\dagger b_{j,r}) P_{j+1}. \end{aligned}$$

Here, the three terms represent, respectively, the nearest-neighbor hopping of an atom in the ground-state level, the nearest-neighbor hopping of an atom in the Rydberg level, and the Rabi coupling between the two levels. The projection operator  $P_j$  projects onto a subspace without an atom in the Rydberg state at each site. Physically, this projection means that the Rydberg excitations of neighboring atoms are energetically prohibited (Fig. 3). We also impose a hard-core constraint, under which each site is occupied by at most one atom.

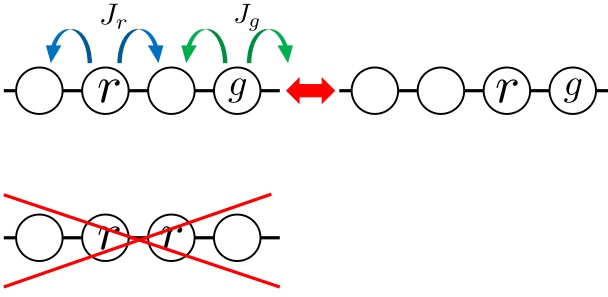


**Fig. 3** : Rydberg-atom chain with hopping on a one-dimensional lattice. Each atom is described as a two-level system consisting of a ground-state level  $g$  and the Rydberg level  $r$ . The Hamiltonian consists of hopping of atoms and the Rabi coupling between the two levels. Here, the Rydberg excitations of neighboring atoms are energetically prohibited.

### 【Results of numerical calculation】

#### (1) Discovery of a series of low-entangled states with high energy

We performed an exact diagonalization of the model introduced above to investigate the distribution of the entanglement entropy of energy eigenstates. In Fig. 4, the horizontal axis represents the energy spectrum, and the vertical axis represents the half-chain entanglement entropy. This figure exhibits a series of low-entangled states with high energy. Such anomalously small entanglement implies that these states violate the eigenstate thermalization hypothesis (ETH) and behave non-thermally. This follows from the fact that the entanglement entropy of a typical state satisfying the ETH exhibits a volume-law scaling like one for the thermodynamic entropy.

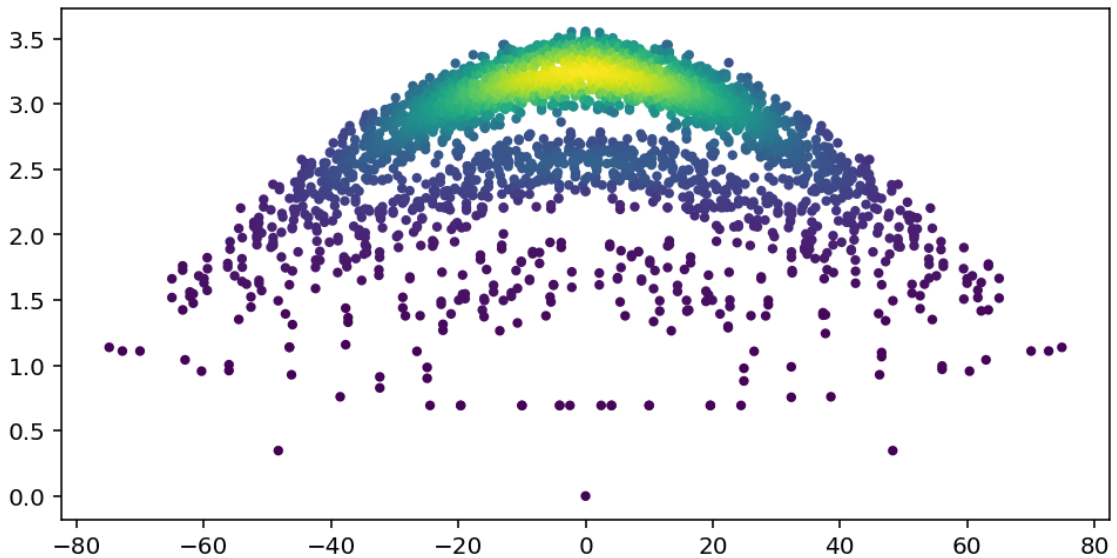


**Fig. 4** : Distribution of the entanglement entropy of energy eigenstates. The horizontal axis represents the energy spectrum, and the vertical axis represents the half-chain entanglement entropy for the system size of  $L = 8$  and the parameters  $J_g = \Omega = 10$  and  $J_r = 1$ . This figure exhibits a series of low-entangled states with high energy.

## (2) Discovery of non-thermalizing dynamics for specific initial states

We observe a nearly constant energy spacing among the above series of low-entangled states. It is well-known that the initial states with a significant overlap with such a series of states do not reach a thermal equilibrium for an anomalously long time. Motivated by this fact, we searched for such non-thermalizing initial states in our model.

We first numerically calculated the time evolution of the fidelity defined as the overlap of the state after time evolution with the initial state. In Fig. 5, the horizontal axis represents the time, and the vertical axis represents the fidelity  $F(t) = |\langle \psi(0) | \psi(t) \rangle|^2$ . Here, the red curve represents the result for an initial state  $\psi(0) = |000r000r\rangle$ , while the green one represents the result for another initial state  $\psi(0) = |00000r0g\rangle$ . The former exhibits revival dynamics while the latter exhibits a fast decay to a value close to zero.

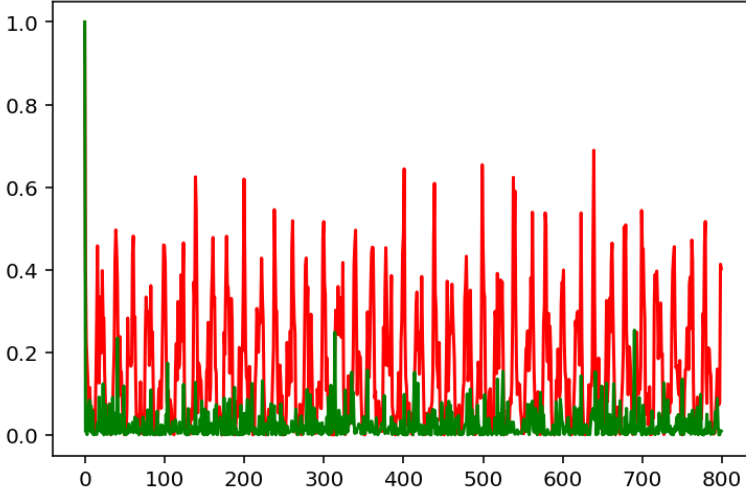


**Fig. 5 :** Time evolution of the fidelity.

The horizontal axis represents the time, and the vertical axis represents the fidelity  $F(t) = |\langle \psi(0) | \psi(t) \rangle|^2$ . Here, the red curve represents the result for an initial state  $\psi(0) = |000r000r\rangle$ , while the green one represents the result for another initial state  $\psi(0) = |00000r0g\rangle$ . The former exhibits revival dynamics while the latter exhibits

a fast decay to a value close to zero.

Then we numerically calculated the time evolution of entanglement for the same set of initial states. In Fig. 6, the horizontal axis represents time, and the vertical axis represents the half-chain entanglement entropy. The red curve exhibits revival to lower values, while the green one exhibits a rapid relaxation to a large value.

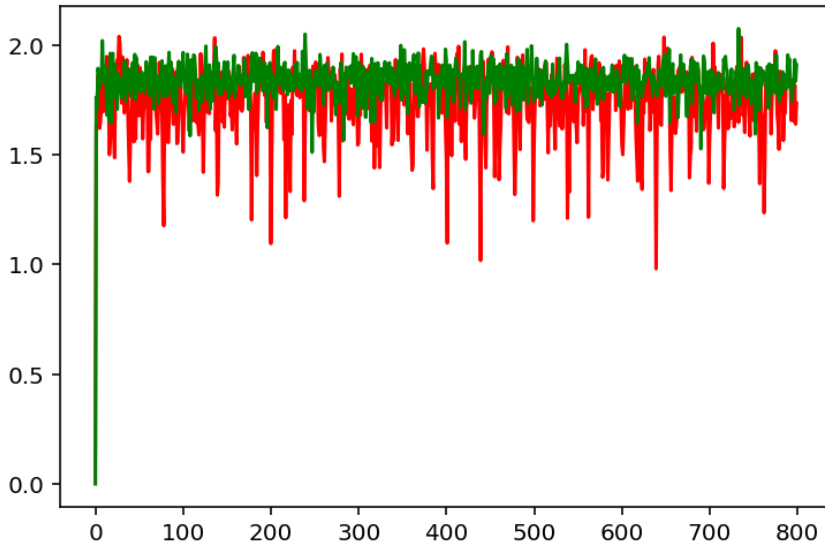


**Fig. 6** : Dynamics of entanglement.

The horizontal axis represents the time, and the vertical axis represents the half-chain entanglement entropy. Here, the red curve represents the result for an initial state  $\psi(0) = |000r000r\rangle$ , while the green one represents the result for another initial state  $\psi(0) = |00000r0g\rangle$ . The former exhibits revival to lower values, while the latter exhibits a rapid relaxation to a large value.

The difference in the dynamics of these two initial states can be understood by examining the distribution of the overlap of them with each energy eigenstate. In Fig. 7, the horizontal axis represents the energy spectrum, and the vertical axis for the scatter plot is the half-chain entanglement entropy. Here, the vertical axis for the bar graphs (colors are consistent with ones in Figs. 5 and 6) represents the distribution of the overlap of the two initial states with each energy eigenstate. The red bars show a significant overlap with a small number of low-entangled states, consistent with revival dynamics. In contrast, the green bars show an almost constant overlap with a large number of energy eigenstates with a wide range of eigenenergy, consistent with rapid relaxation.

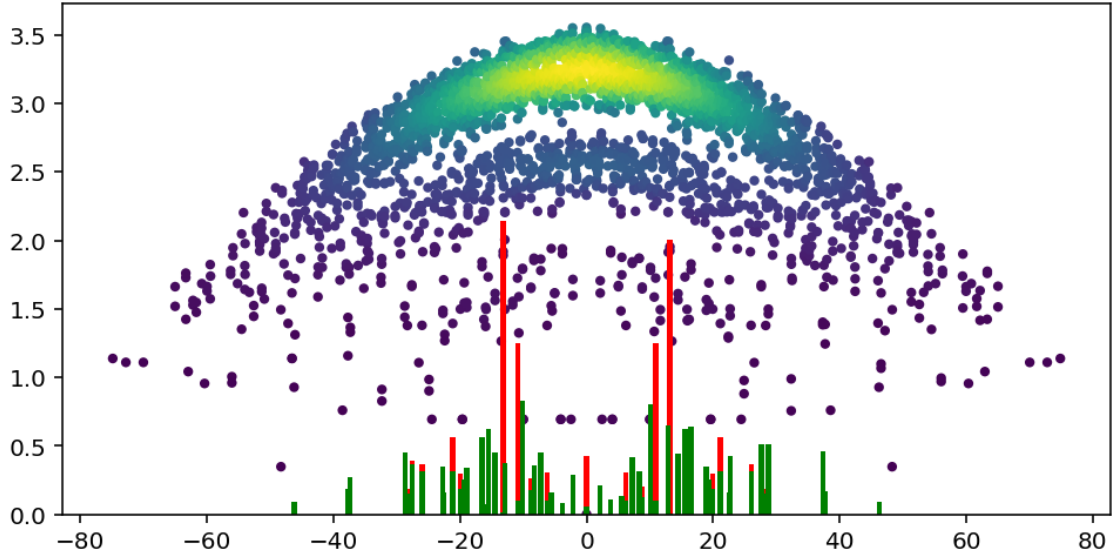


**Fig. 7** : Distribution of the overlap of the two initial states with each energy eigenstate. The horizontal axis represents the energy spectrum, and the vertical axis for the scatter plot represents the half-chain entanglement entropy. Here, the vertical axis for the bar graphs represents the distribution of the overlap of the two initial states with each energy eigenstate. The red bars represent the result for an initial state  $\psi(0) = |\mathbf{000r000r}\rangle$ , while the green ones represent the result for another initial state  $\psi(0) = |\mathbf{00000r0g}\rangle$ . The red bars show a significant overlap with a small number of low-entangled states, while the green ones show an almost constant overlap with a large number of energy eigenstates with a wide range of eigenenergy.

### 【Mathematical Analysis】

In addition to numerical calculation of the dynamics, we have clarified explicit expressions of some simple quantum many-body scar states.

#### (1) Explicit expressions of single-particle quantum many-body scar states

We have found the following expression of single-particle states:

$$|\pm, k\rangle \propto (b_{k,r}^\dagger \pm b_{k,g}^\dagger) |\text{vac}\rangle.$$

This state is a simultaneous eigenstate of the three parts of the Hamiltonian with the eigenenergy



$$E = \pm \Omega - 2 (J_g + J_r) \cos k.$$

Furthermore, this state has the half-chain entanglement entropy of  $\log 2$  and is included in the series of low-entangled states.

## (2) Explicit expressions for two-particle quantum many-body scar states

As a concrete example of simple two-particle quantum many-body scar states, we consider the following translational-invariant bound state:

$$|s_1, s_2, k \rangle \propto \sum_j e^{ikj} (b_{j+2,r}^\dagger + s_1 b_{j+2,g}^\dagger) (b_{j,r}^\dagger + s_2 b_{j,g}^\dagger) |\text{vac} \rangle.$$

We have found that this state is an eigenstate of the hopping terms  $H_g + H_r$  only for the momentum  $k = \pi$ , while this state is an eigenstate of  $H_{Rabi}$  for a general value of  $k$ . Such bound states with the wavenumber  $k = \pi$  are formally similar to the eta-pairing states in the Hubbard model [6].

## 【Conclusion】

This research has numerically and analytically explored the effects of hopping on the quantum many-body scar states in a Rydberg-atom chain. As a result, we have found that new quantum many-body scar states with an anomalously small entanglement emerge by adding the hopping degree of freedom. Furthermore, we have found new non-thermalizing initial states exhibiting revival dynamics for the fidelity and the entanglement. In addition to numerical calculation, we have found explicit expressions for some simple quantum many-body scar states. The present study provides insights into quantum many-body scar states and thermalization from a more general viewpoint than before.

## 【Outlook for future developments】

### (1) Numerical analysis with partitioning into symmetry sectors

In the numerical calculation in this study, we have analyzed the whole Hilbert space without dividing it into symmetry sectors. In future work, the influence of such symmetry will be understood explicitly by studying the behavior within each symmetry sector.

### (2) Investigation into revival dynamics in many-particle states

This study has focused on the time evolution of states with a small number of particles and has

found initial states that do not reach thermal equilibrium. In future work, more non-trivial results arising from significant contribution of interaction will be obtained by investigating similar non-thermalizing dynamics in states with a large number of particles.

### (3) Explicit expressions and algebraic structures in many-particle scar states

This work has focused on quantum many-body scar states with a small number of particles and clarified explicit expressions. In future work, it is worthwhile to search for expressions and algebraic structures that can be generalized to cases involving a large number of particles.

### 【Acknowledgement】

We are grateful to our supervisors Prof. H. Katsura and Prof. M. Ueda for their support and cooperation in carrying out this research. We also thank our MERIT advisors, Prof. M. Fujita and Prof. Y. Nakamura for their advice and approval of our proposal. Finally, we are grateful to the MERIT program for providing us with an opportunity for the self-directed joint research.

### 【References】

- [1] S. Trotzky *et al.*, *Nat. Phys.*, **8**, 325 (2012)
- [2] M. Srednicki, *Phys. Rev. E* **50**, 888 (1994); M. Rigol *et al.*, *Nature* **452**, 854 (2008)
- [3] L. D'Alessio *et al.*, *Adv. Phys.* **65**, 239 (2016)
- [4] H. Bernien *et al.*, *Nature* **551**, 579 (2017)
- [5] C. J. Turner *et al.*, *Nat. Phys.* **14**, 745 (2018)
- [6] C. N. Yang, *Phys. Rev. Lett.* **63**, 2144 (1989)